Clinical trials with combination therapy for cancer: how to design them effectively

Avner Friedman

Ohio State University

Contents

- Why most clinical trials fail?
- Mathematical models can suggest how to better conduct such trials
- One detailed example, including a PDE system with a free boundary, and estimated parameters
- Other examples more briefly

Clinical trials failure

- Most positive phase II clinical trials with combination therapy fail in phase III
- The failure is partly due to the fact that not sufficient forethought is given to the interaction that may take place between the diverse agents
- If there is antagonism between the two agents, how to schedule the protocol in order to reduce it ?
- How reduce negative side-effect without compromising efficacy of treatment ?
- We can use mathematical models and simulations to address these questions

The mathematics involved in the model

The mathematical models are given by a system of PDEs in the tumor region, and the tumor boundary is a free boundary, one of the unknown of the problem

A network is introduced which is only ‘as large as necessary’ in order to address the question

The main effort is then to estimate the parameters, simulate the model and perform sensitivity analysis

I will give one example in detail

PLOS ONE

RESEARCH ARTICLE

Combination therapy for cancer with oncolytic virus and checkpoint inhibitor: A mathematical model

Avner Friedman[1], **Xiulan Lai**[2]*

1 Mathematical Bioscience Institute & Department of Mathematics, Ohio State University, Columbus, OH, United States of America, **2** Institute for Mathematical Sciences, Renmin University of China, Beijing, P. R.

February 2018

T cells kill cancer cells but they have checkpoints . Checkpoint inhibitor drugs are now in use in clinical treatment of cancer

CTLA-4 is a receptor on T cells and B7 is a ligand on dendritic cells. The complex CTLA-4 –B7 blocks the activities of T cells; anti-CTLA-4 is anti-cancer drug

PD-1 is a receptor on T cells and PD-L1 is a ligand on tumor cells (and also on T cells). The complex PD-1 ---PD-L1 blocks the activities of the T cells; anti-PD-1 is anti-cancer drug

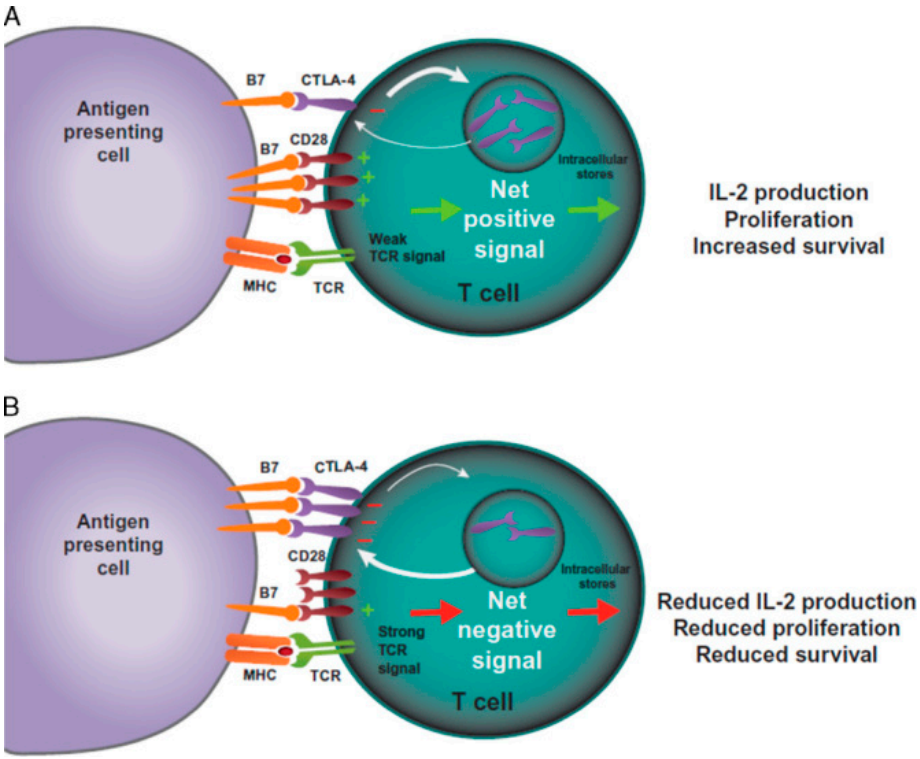

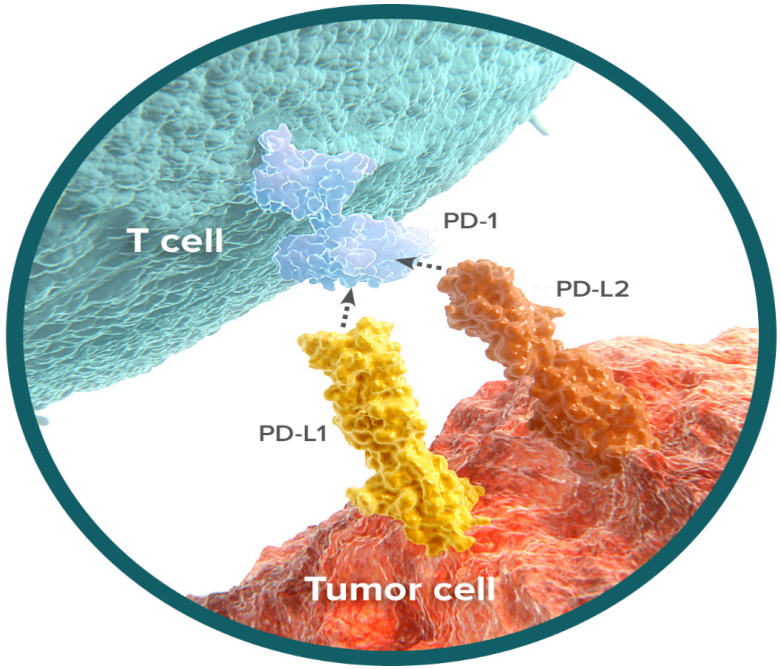

Oncolytic virus

Oncolytic virus is a genetically modified virus that can invade cancer cells but not normal healthy cells

When the virus-infected cancer cell dies, the released virus particles proceed to infected more cancer cells

Table 1. List of variables (in units of g/cm^3).

Notation	Description	Notation	Description
C	density of cancer cells	T_8	density of activated CD8$^+$ T cells
C_i	density of infected cancer cells	I_{12}	IL-12 concentration
V Drug	density of extracellular virus	I_2	IL-2 concentration
V_i	density of intracellular virus	P	PD-1 concentration
M	density of macrophages	L	PD-L1 concentration
D	density of dentritic cells	Q	PD-1-PD-L1 concentration
T_1	density of activated CD4$^+$ T cells	A Drug	anti-PD-L1 concentration

When PD-L1 combine with PD-1 receptor on effector T cells , the T cells activity is reduced

Anti-PD-1 is anti-cancer drug. Oncolytic virus is also used as anti-cancer drug

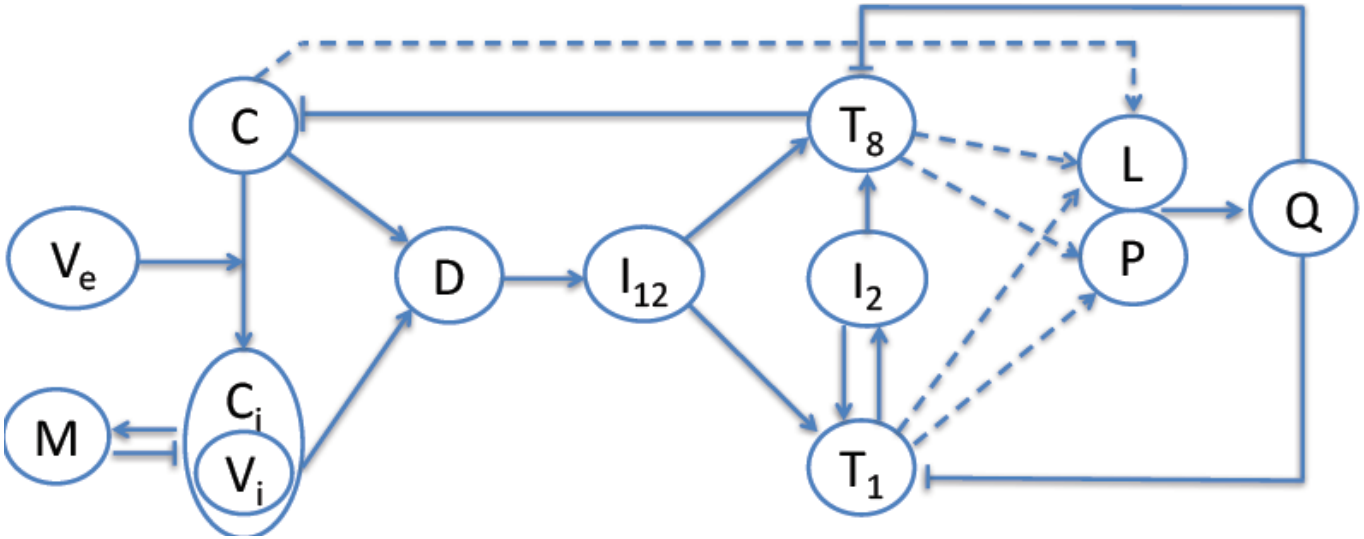

$$C + C_i + M + D + T_1 + T_8 = \text{constant} = \theta. \tag{1}$$

$$\frac{\partial C}{\partial t} + \nabla \cdot (\mathbf{u}C) - \delta_C \nabla^2 C = \underbrace{\lambda_C C\left(1 - \frac{C}{C_M}\right)}_{\text{growth}} - \underbrace{\beta_C C V_e}_{\text{infection by } V_e} - \underbrace{\eta_8 T_8 C}_{\text{killed by CD8}^+ \text{ T cells}} - \underbrace{d_C C}_{\text{death}}, \tag{2}$$

$$\frac{\partial C_i}{\partial t} + \nabla \cdot (\mathbf{u}C_i) - \delta_{C_i} \nabla^2 C_i = \beta_C C V_e - \underbrace{d_C(1 + \mu_{V_i} V_i) C_i}_{\text{death}} - \underbrace{\mu_{C_i M} C_i M}_{\text{killed by } M} - \underbrace{\eta_{8C_i} T_8 C_i}_{\text{killed by CD8}^+ \text{ T cells}}. \tag{3}$$

$$\frac{\partial V_e}{\partial t} - \delta_{V_e} \nabla^2 V_e = \sum_{j=1}^{m} \gamma_V \delta(t - t_j) + \underbrace{N d_C (1 + \mu_{V_i} V_i) V_i}_{\text{released by } C_i \text{ death}} - \underbrace{\beta_V C V_e}_{V_e \to V_i} - \underbrace{\mu_{V_e M} M V_e}_{\text{endocytosed by } M}, \tag{4}$$

T cells killing of infected cancer cell is pro-cancer

Injection of virus at successive days

$$\frac{\partial V_i}{\partial t} + \nabla \cdot (\mathbf{u} V_i) - \delta_{C_i} \nabla^2 V_i = \underbrace{\beta_V C V_e}_{V_e \to V_i} + \underbrace{\lambda_{V_i} C_i}_{\text{growth of } V_i \text{ in } C_i} - \underbrace{N d_C (1 + \mu_{V_i} V_i) V_i}_{\text{released through death of } C_i}$$
$$- \underbrace{\mu_{C_i M} V_i M}_{\text{killed by } M} - \underbrace{\eta_{8C_i} T_8 V_i}_{\text{killed by CD8}^+ \text{ cells}} . \qquad (5)$$

Vi grows in Ci

$$\frac{\partial M}{\partial t} + \nabla \cdot (\mathbf{u} M) - \delta_M \nabla^2 M = \underbrace{\lambda_M}_{\text{Source}} + \underbrace{\lambda_{MC_i} M C_i}_{\text{growth}} - \underbrace{d_M M}_{\text{death}}, \qquad (6)$$

$$\frac{\partial D}{\partial t} + \underbrace{\nabla \cdot (\mathbf{u} D)}_{\text{velocity}} - \underbrace{\delta_D \nabla^2 D}_{\text{difusion}} = \underbrace{\lambda_{DV} D_0 V_i}_{\text{activation by intracellular virus}}$$
$$+ \underbrace{\lambda_{DC} D_0 \frac{C}{K_C + C}}_{\text{activation by HMGB-1}} - \underbrace{d_D D}_{\text{death}}, \qquad (7)$$

$$\frac{\partial T_1}{\partial t} + \nabla \cdot (\mathbf{u} T_1) - \delta_T \nabla^2 T_1 = \underbrace{\left(\hat{\lambda}_{T_1 I_{12}} T_{10} \frac{I_{12}}{K_{I_{12}} + I_{12}} \frac{D}{K_D + D} \right.}_{\text{activation by IL-12}} + \underbrace{\left. \lambda_{T_1 I_2} T_1 \frac{I_2}{K_{I_2} + I_2} \right)}_{\text{promotion by IL-2}}$$

$$\times \underbrace{\frac{1}{1 + Q/K_{TQ}}}_{\text{inhibition by PD-1-PD-L1}} - \underbrace{d_{T_1} T_1}_{\text{death}} . \tag{8}$$

$$\frac{\partial T_8}{\partial t} + \nabla \cdot (\mathbf{u} T_8) - \delta_T \nabla^2 T_8 = \underbrace{\left(\hat{\lambda}_{T_8 I_{12}} T_{80} \frac{I_{12}}{K_{I_{12}} + I_{12}} \frac{D}{K_D + D} \right.}_{\text{activation by IL-12}} + \underbrace{\left. \lambda_{T_8 I_2} T_1 \frac{I_2}{K_{I_2} + I_2} \right)}_{\text{promotion by IL-2}}$$

$$\times \underbrace{\frac{1}{1 + Q/K_{TQ}}}_{\text{inhibition by PD-1-PD-L1}} - \underbrace{d_{T_8} T_8}_{\text{death}} . \tag{9}$$

$$\frac{\partial I_{12}}{\partial t} - \delta_{I_{12}} \nabla^2 I_{12} = \underbrace{\lambda_{I_{12} D} D}_{\text{production by DCs}} - \underbrace{d_{I_{12}} I_{12}}_{\text{degradation}} . \tag{10}$$

$$\frac{\partial I_2}{\partial t} - \delta_{I_2} \nabla^2 I_2 = \underbrace{\lambda_{I_2 T_1} T_1}_{\text{production by } T_1} - \underbrace{d_{I_2} I_2}_{\text{degradation}} . \tag{11}$$

Inhibitio
by Q

$$\frac{\partial P}{\partial t}+\nabla\cdot(\mathbf{u}P_1)-\delta_T\nabla^2P=\frac{P}{T_1+T_8}\left[(\lambda_{T_1I_{12}}T_{10}+\lambda_{T_8I_{12}}T_{80})\frac{I_{12}}{K_{I_{12}}+I_{12}}+(\lambda_{T_1I_2}T_1+\lambda_{T_8I_2}T_8)\frac{I_2}{K_{I_2}+I_2}\right]\times\frac{1}{1+Q/K_{TQ}}$$
$$-\frac{P}{T_1+T_8}(d_{T_1}T_1+d_{T_8}T_8)-\underbrace{\mu_{PA}PA}_{\text{depletion by anti-PD-1}}. \tag{12}$$

$$L=\rho_L(T_1+T_8+\varepsilon C), \qquad P+L\underset{d_Q}{\overset{\alpha_{PL}}{\rightleftharpoons}}Q. \qquad Q=\sigma PL,$$

Anti-PD-1

$$\frac{\partial A}{\partial t}-\delta_A\nabla^2A=\underbrace{\sum_{j=1}^{''}\gamma_AH(t-t_j)e^{-\alpha(t-t_j)}}_{\text{injection}}-\underbrace{\mu_{AP}PA}_{\text{depletion through blocking PD-1}}$$
$$-\underbrace{d_AA}_{\text{degradation}}. \tag{16}$$

Injection and depletion

Velocity of cells

$$0.6034\times\nabla\cdot\mathbf{u}=\text{RHS of Eq (2)}+\text{RHS of Eq (3)}+\sum_{j=6}^{9}[\text{RHS of Eq (j)}]. \tag{17}$$

Equation for free boundary (R): We assume that the free boundary $r = R(t)$ moves with the velocity of cells, so that

$$\frac{dR(t)}{dt} = u(R(t), t). \tag{18}$$

Boundary conditions

$$\frac{\partial T_8}{\partial n} + \sigma_T(I_{12})(T_8 - \hat{T}_8) = 0, \quad \frac{\partial T_1}{\partial n} + \sigma_T(I_{12})(T_1 - \hat{T}_1) = 0 \quad \text{at } r = R(t), \tag{19}$$

where $\sigma_T(I_{12}) = \alpha_T \frac{I_{12}}{K_{I_{12}} + I_{12}} \frac{D}{K_D + D}$.

$$\text{zero-flux for } C,\ C_i,\ V_e,\ V_i,\ M,\ D,\ I_{12},\ I_2,\ P,\ A(r,t) \quad \text{at } r = R(t). \tag{20}$$

Table 2. Summary of parameter values.

Notation	Description	Value used	References
δ_D	diffusion coefficient of DCs	8.64×10^{-7} cm^2 day^{-1}	[38]*
δ_{T_1}	diffusion coefficient of CD4$^+$ T cells	8.64×10^{-7} cm^2 day^{-1}	[38]*
δ_{T_8}	diffusion coefficient of CD8$^+$ T cells	8.64×10^{-7} cm^2 day^{-1}	[38]*
δ_C	diffusion coefficient of tumor cells	8.64×10^{-7} cm^2 day^{-1}	[38]*
δ_M	diffusion coefficient of macrophages	8.64×10^{-7} cm^2 day^{-1}	[38]*
$\delta_{I_{12}}$	diffusion coefficient of IL-12	6.0472×10^{-2} cm^2 day^{-1}	[39]
δ_{I_2}	diffusion coefficient of IL-2	9.9956×10^{-2} cm^2 day^{-1}	[39]
δ_A	diffusion coefficient of IL-2	4.73×10^{-2} cm^2 day^{-1}	[39]
α_T	flux rate of T cells on the boundary	1 cm^{-1}	estimated
λ_C	growth rate of cancer cells	0.65 day^{-1}	estimated
λ_{V_i}	growth rate of intracellular virus	6×10^{-4} day^{-1}	estimated
λ_M	growth rate of macrophages	0.009 day^{-1}	[51]*
λ_{MC_i}	activation rate of macrophages by C_i	0.04 cm^3/g	estimated
λ_{DV}	activation rate of DCs by virus infection	5.2×10^{10} cm^3/g · day	estimated
λ_{DC}	activation rate of DCs by tumor cells	5.2 day^{-1}	estimated
$\lambda_{T_1 I_{12}}$	activation rate of CD4$^+$ T cells by IL-12	9.32 day^{-1}	[39]
$\lambda_{T_1 I_2}$	activation rate of CD4$^+$ T cells by IL-2	0.25 day^{-1}	[39]

$\lambda_{T_1 I_2}$	activation rate of $CD4^+$ T cells by IL-2	0.25 day^{-1}	[39]
$\lambda_{T_8 I_{12}}$	activation rate of $CD8^+$ T cells by IL-12	8.30 day^{-1}	[39]
$\lambda_{T_8 I_2}$	activation rate of $CD8^+$ T cells by IL-2	0.25 day^{-1}	[39]
$\lambda_{I_{12} D}$	production rate of IL-12 by DCs	2.76×10^{-6} day^{-1}	[39]
$\lambda_{I_2 T_1}$	production rate of IL-2 by $CD4^+$ T cells	2.82×10^{-8} day^{-1}	[39]
β_C	infection rate of cancer cells by virus	9×10^4 $cm^3/g \cdot day$	estimated
β_V	rate of transition from V_e to V_i by infection	0.09 $cm^3/g \cdot day$	estimated
$\mu_{C_i M}$	killing rate of C_i by M	4.8×10^{-2} $cm^3/g \cdot day$	estimated
$\mu_{V_e M}$	clearance rate of V_e by M	2 $cm^3/g \cdot day$	estimated
μ_{V_i}	death rate of infected cell due to viral burden	5×10^7 day^{-1}	estimated
N	burst size of V_i from natural death of C_i	100	estimated
η_8	killing rate of tumor cells by $CD8^+$ T cells	1.38×10^2 $day^{-1} \cdot cm^3/g$	estimated
η_{8C_i}	killing rate of infected cancer cells by $CD8^+$ T cells	7.59×10^3 $day^{-1} \cdot cm^3/g$	estimated
μ_{PA}	blocking rate of PD-1 by anti-PD-1	6.87×10^4 $cm^3/g \cdot day$	[39]
ρ_P	expression of PD-1 in T cells	2.49×10^{-7}	[39]
ρ_L	expression of PD-L1 in T cells	5.22×10^{-7}	[39]
ε	relative expression of PD-L1 in tumor cells	0.01	[39]
d_C	death rate of uninfected tumor cells	0.17 day^{-1}	[50]*
d_M	death rate of macrophages	0.015 day^{-1}	[51]
d_D	death rate of DCs	0.1 day^{-1}	[50]
d_{T_1}	death rate of $CD4^+$ T cells	0.197 day^{-1}	[50]
d_{T_8}	death rate of $CD8^+$ T cells	0.18 day^{-1}	[50]
$d_{I_{12}}$	degradation rate of IL-12	1.38 day^{-1}	[50]
d_{I_2}	degradation rate of IL-2	2.376 day^{-1}	[50]

Table 3. Summary of parameter values.

K_C	half-saturation of tumor cells	$0.4\ g/cm^3$	[50]
K_D	half-saturation of DCs	$0.4 \times 10^{-4}\ g/cm^3$	[39]
$K_{I_{12}}$	half-saturation of IL-12	$1.5 \times 10^{-10}\ g/cm^3$	[50]
K_{I_2}	half-saturation of IL-2	$2.37 \times 10^{-11}\ g/cm^3$	[50]
K_{T_1}	half-saturation of $CD4^+$ T cells	$2 \times 10^{-3}\ g/cm^3$	[39]
K_{T_8}	half-saturation of $CD8^+$ T cells	$1 \times 10^{-3}\ g/cm^3$	[39]
K'_{TQ}	inhibition of function of T cells by PD-1-PD-L1	$1.365 \times 10^{-18}\ g/cm^3$	[39]*
θ	total cell density	$0.6034\ g/cm^3$	**
D_0	density of immature DCs	$2 \times 10^{-5}\ g/cm^3$	[50]
T_{10}	density of naive $CD4^+$ T cells	$4 \times 10^{-4}\ g/cm^3$	[39]*
T_{80}	density of naive $CD8^+$ T cells	$2 \times 10^{-4}\ g/cm^3$	[39]*
C_M	carrying capacity of cancer cells	$0.8\ g/cm^3$	[50]
$\hat{T}_1$	density of $CD4^+$ T cells from lymph node	$4 \times 10^{-3}\ g/cm^3$	[39]*
$\hat{T}_8$	density of $CD8^+$ T cells from lymph node	$2 \times 10^{-3}\ g/cm^3$	[39]*

* In this reference the value was estimated but not obtained directly from experimental results.

** The value is determined by Eq (1) with steady state densities of the cells.

Methods for estimating parameters are explained, with examples, in Chapter 5 of this recent monograph

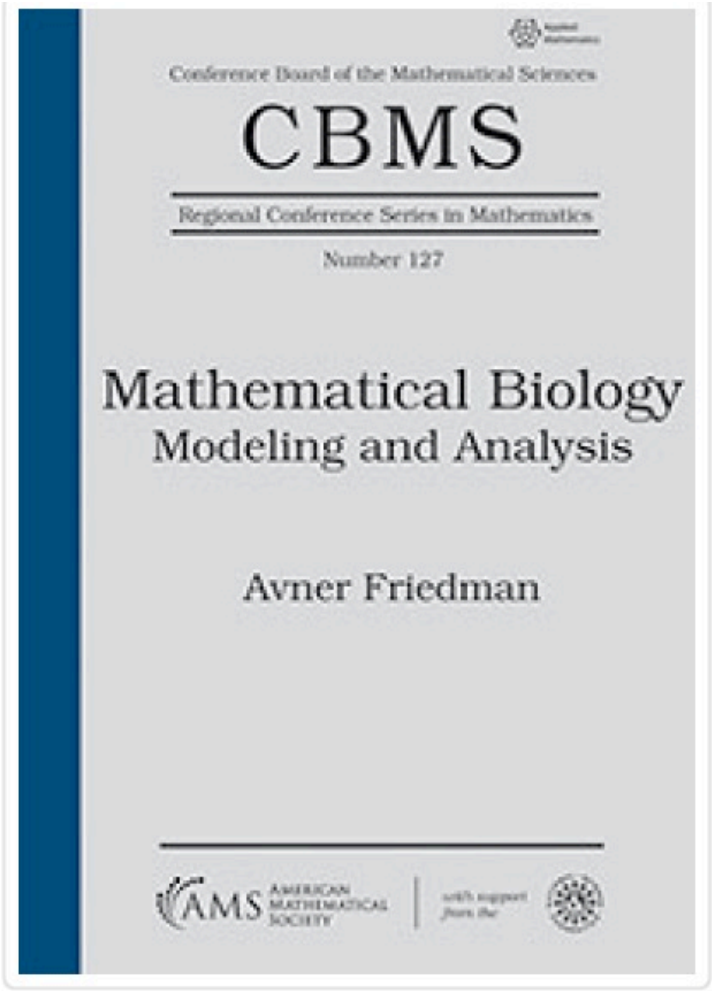

Control case

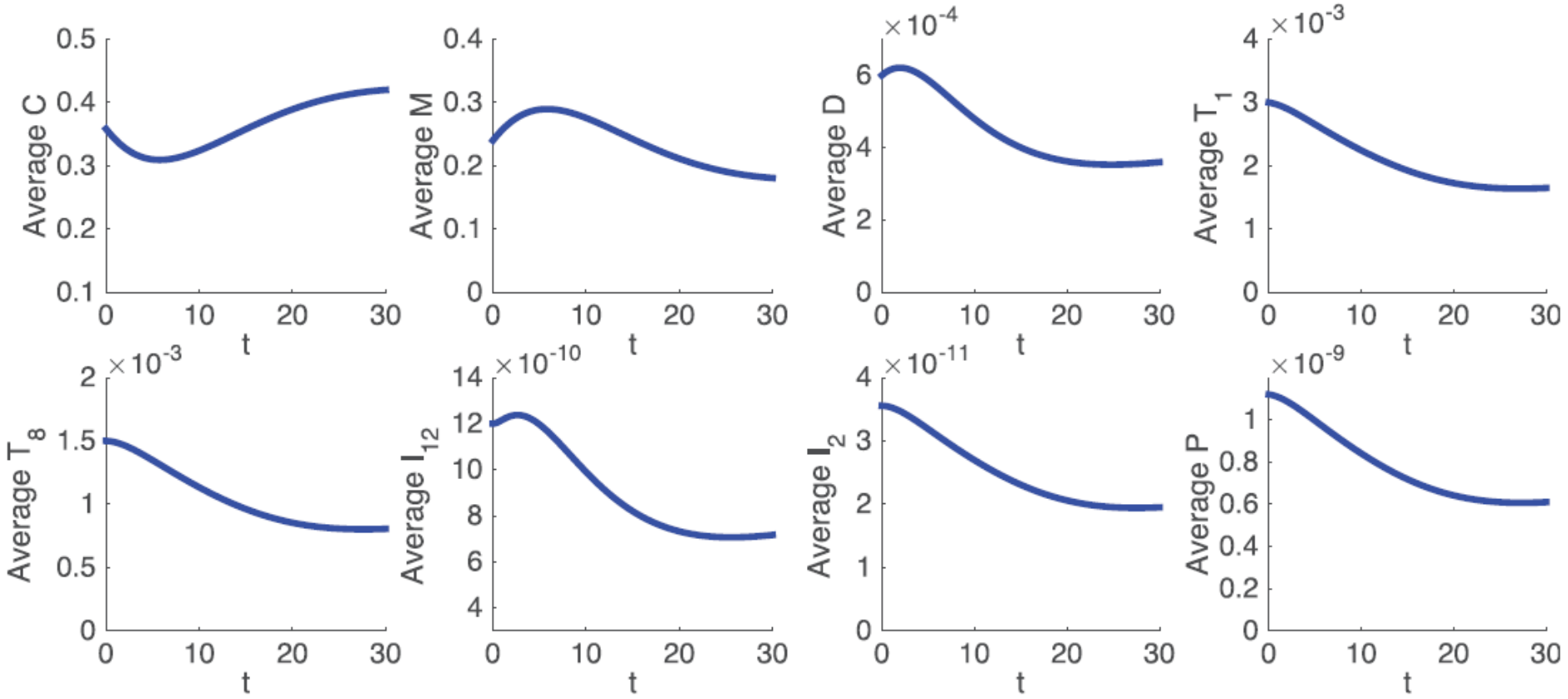

Fig 2. Average densities/concentrations, in g/cm^3, of all the variables in the model in the control case. All parameter values are the same as in Tables 2 and 3. Initial values are as in (21).

Sensitivity analysis

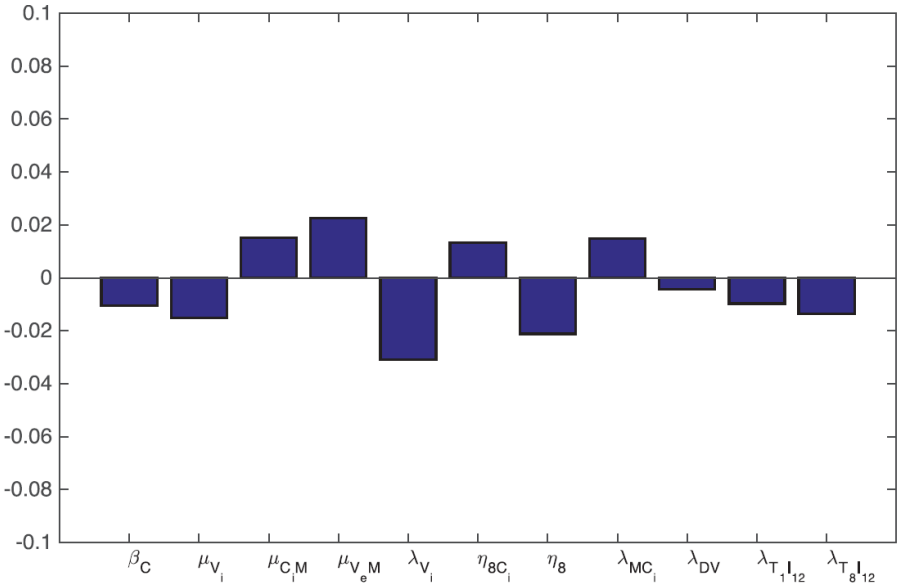

Fig 9. Statistically significant PRCC values (p-value< 0.01) for $R(t)$ at day 60.

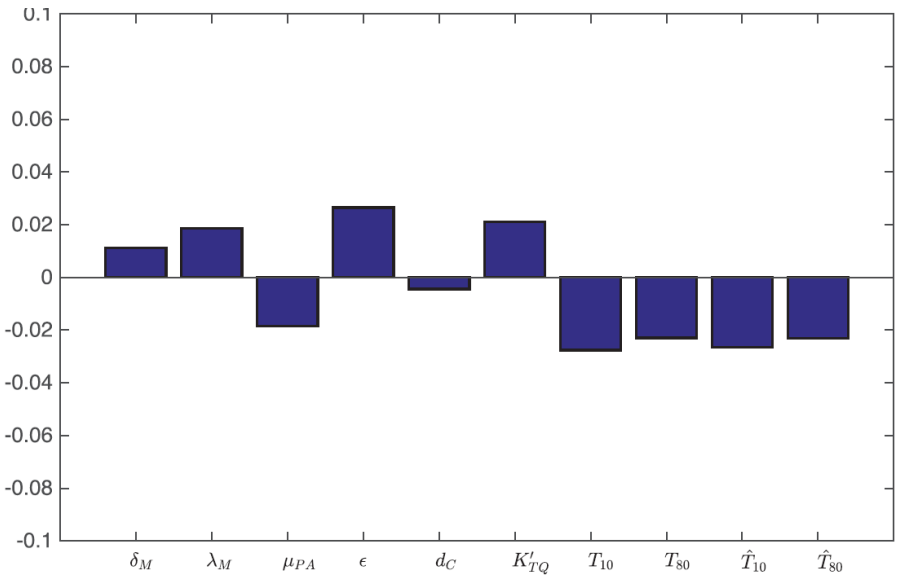

Fig 8. Statistically significant PRCC values (p-value< 0.01) for $R(t)$ at day 60.

Qualitative agreement with mice models

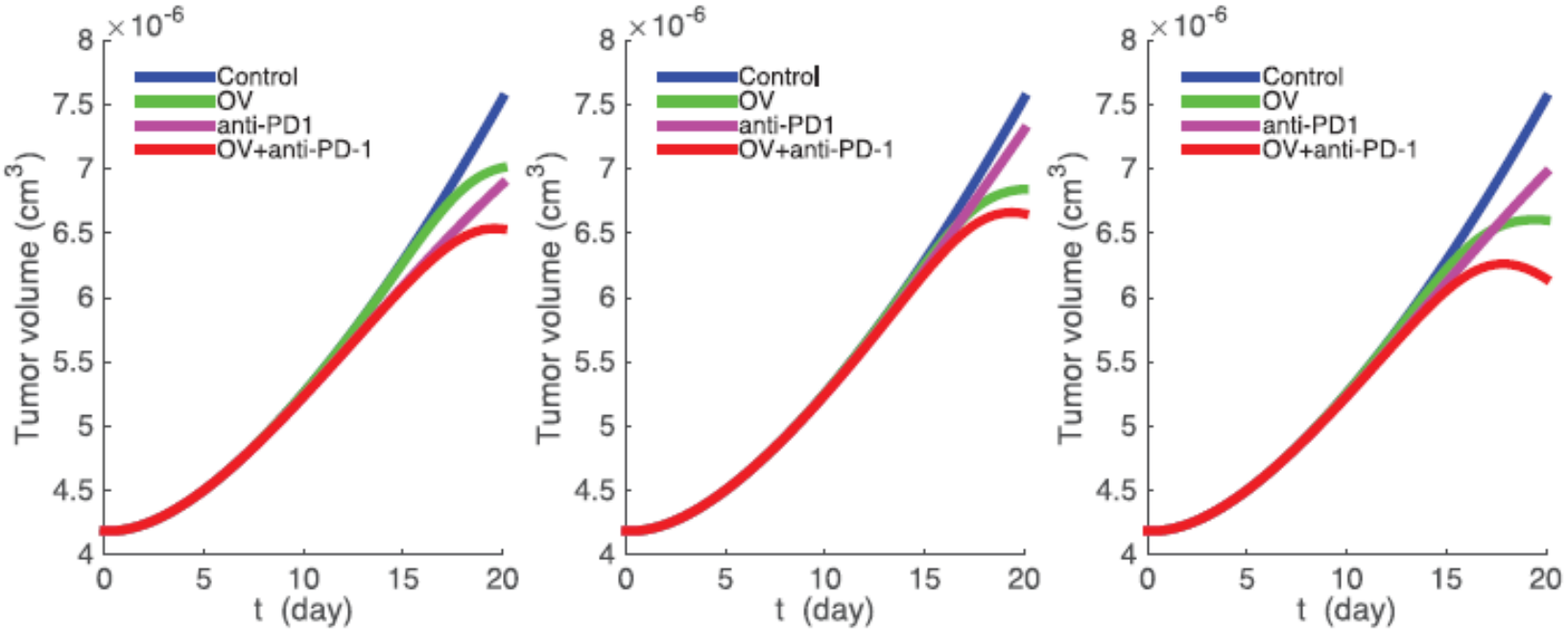

Fig 3. The growth of tumor volume. OV is given at days $t = 0, 2, 4$ with the amount γ_V and anti-PDE-1 is given at days $t = 4, 7, 11$ with the amount γ_A. (a) $\gamma_V = 0.1 \times 10^{-10}$ g/cm^3, $\gamma_A = 8 \times 10^{-7}$ g/cm^3. (b) $\gamma_V = 0.2 \times 10^{-10}$ g/cm^3, $\gamma_A = 3 \times 10^{-7}$ g/cm^3. (c) $\gamma_V = 0.5 \times 10^{-10}$ g/cm^3, $\gamma_A = 7 \times 10^{-7}$ g/cm^3. Parameter values are the same as in Fig 2.

The two drugs, anti-PD-1 and oncolytic therapy may be antagonistic:

Anti-PD-1 increases the killing rate by T cells of cancer cells, including those infected with virus, so this may not necessarily be a good thing, since the virus is also killing cancer cells

Antagonism

Efficacy $E(\gamma_V, \gamma_A) = \dfrac{V_{24}(0,0) - V_{24}(\gamma_V, \gamma_A)}{V_{24}(0,0)}$;

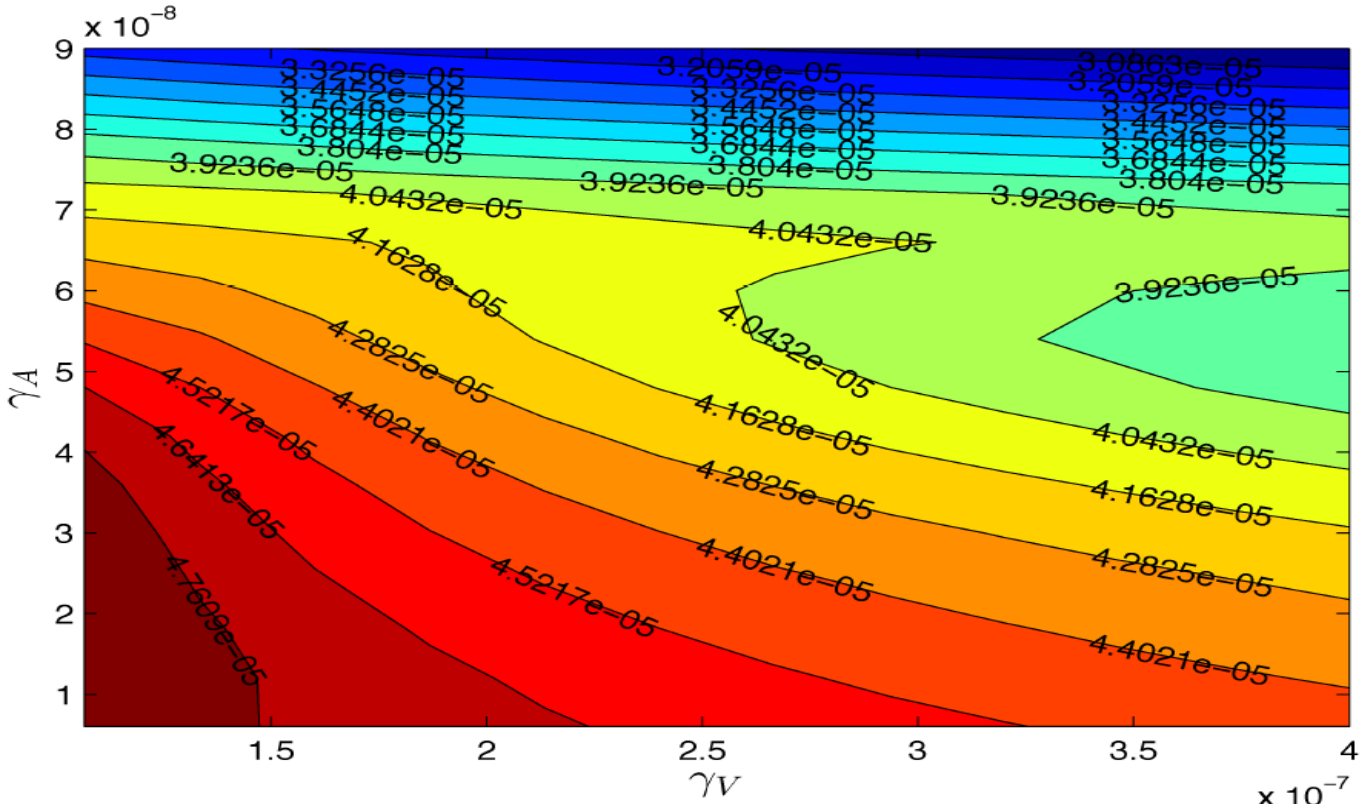

We marked the tumor volume on the equi-efficacy curves

Conclusion

Avoid “zones of antagonism”: for some values of γ_V or of viral growth in cancer cells λ_V, an increase in the dose γ_A actually increases the tumor volume------

”more is not always better”

BET inhibitor

The BET family proteins perform transcriptional regulatory function for many genes, including oncogenes

For this reason, BET inhibitor is being studied in mice experiments as anti-cancer drug

Combination therapy for breast cancer with BET inhibitor and immune checkpoint inhibitor: A mathematical model

Xiulan Lai[a], Andrew Stiff[b], Megan Duggan[c], Robert Wesolowski[d], William E. Carson III[e], and Avner Friedman[f,1]

PNAS June 2018

B7 on dendritic cells combine with CTLA on effective T cell to block toxic T cell activity

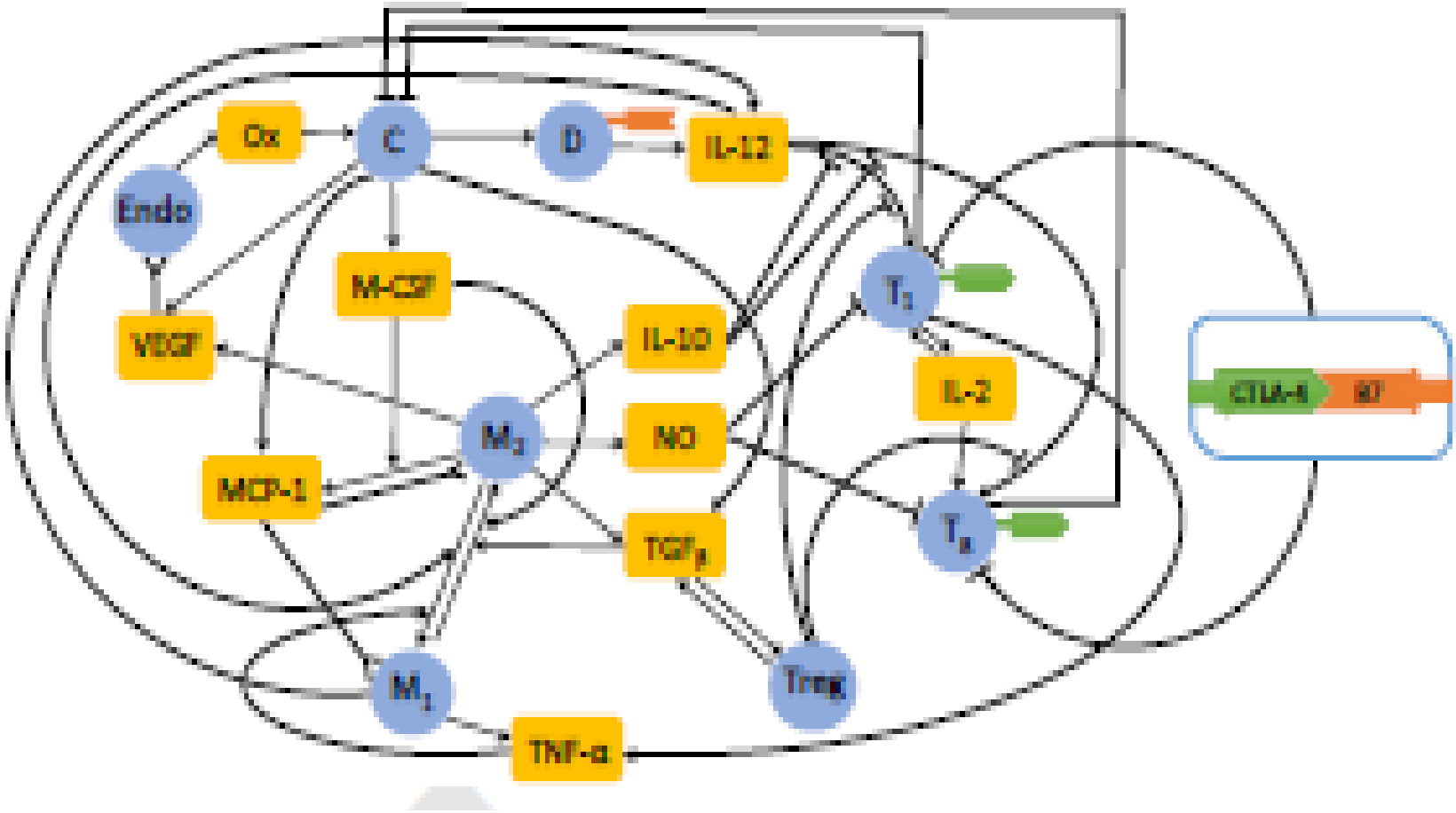

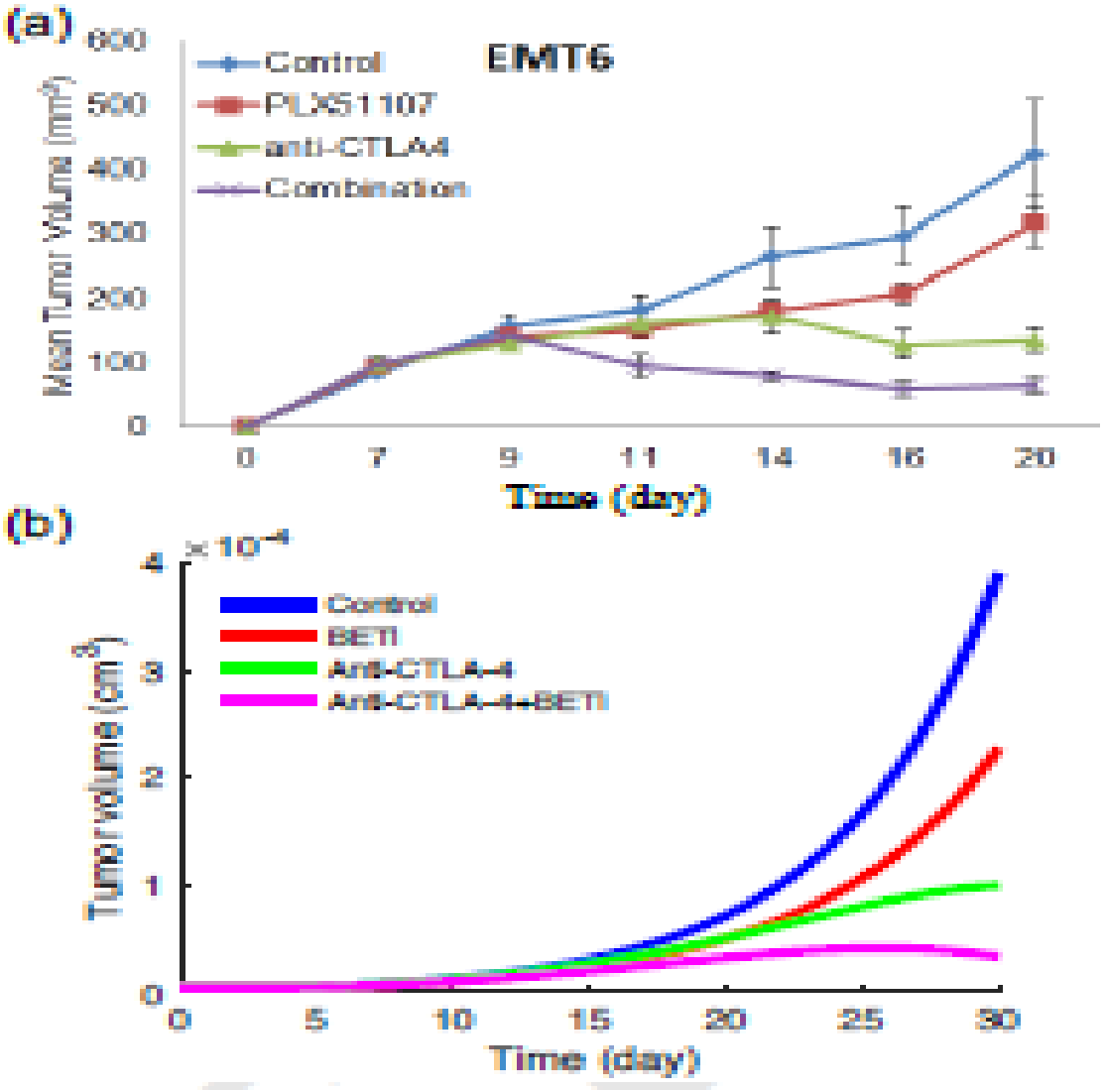

Breast cancer in mice

Negative side effects

Cancer treatment may give rise to negative side effects, for example, to increase in the inflammatory cytokine TNF - alpha

$$E(\gamma_B, \gamma_A) = \frac{V_{30}(0,0) - V_{30}(\gamma_B, \gamma_A)}{V_{30}(0,0)},$$

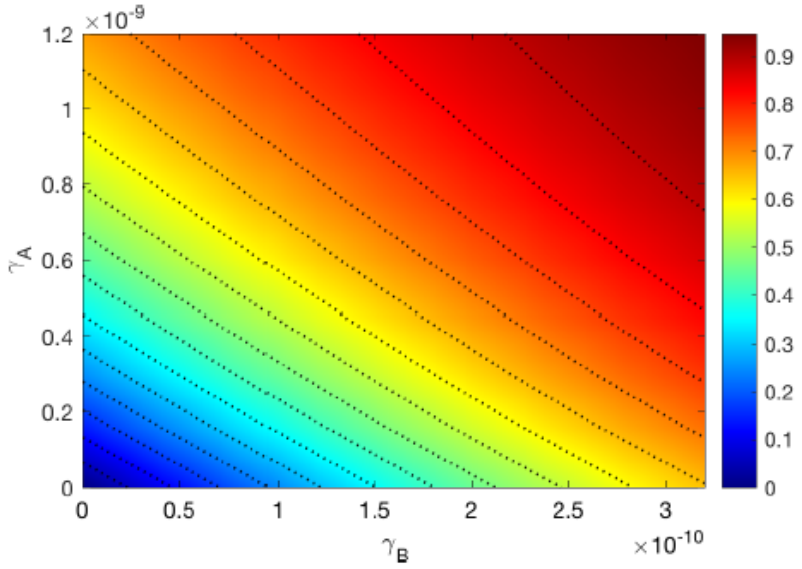

Fig. 4. **Drug efficacy map.** The color column shows the efficacy $E(\gamma_B, \gamma_A)$ when γ_B varies between $0 - 0.32 \times 10^{-9}$ g/cm^3 · day and γ_A varies between $0 - 1.2 \times 10^{-9}$ g/cm^3 · day. All other parameter values are the same as in Tables S2, S3 and S4.

$$AE(\gamma_B, \gamma_A) = \frac{T\alpha_{30}(\gamma_B, \gamma_A) - T\alpha_{30}(0,0)}{T\alpha_{30}(0,0)}.$$

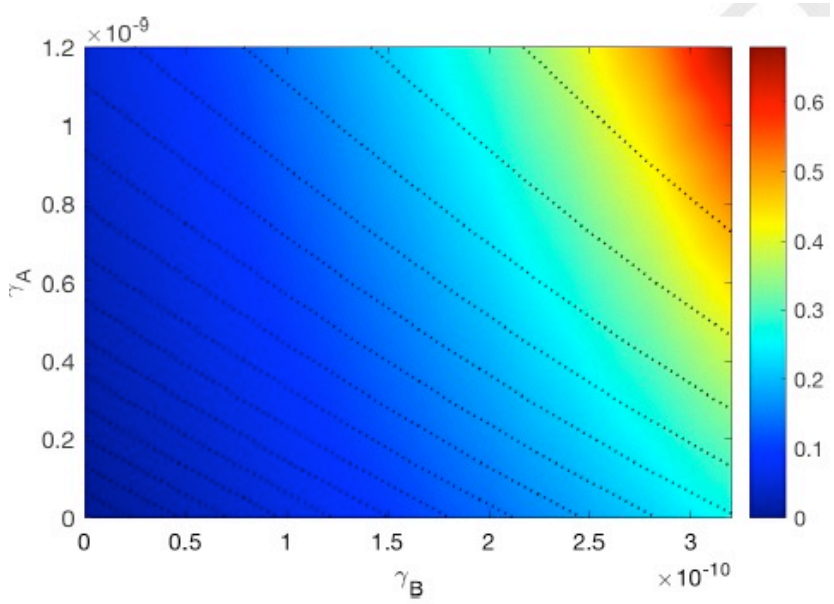

Fig. 5. **Average density of TNF-α.** The color column shows the 'adverse effect' function $AE(\gamma_B, \gamma_A)$ when γ_B varies between $0 - 0.32 \times 10^{-9}$ g/cm^3 · day and γ_A varies between $0 - 1.2 \times 10^{-9}$ g/cm^3 · day. All other parameter values are the same as in Tables S2, S3 and S4.

Conclusion

One can achieve the same tumor reduction with many different amounts of BETi and anti-CTLA-4 inhibitor, but the best choice that will reduce TNF-alpha (and the associated gastro-intestinal reaction) is to take the pair with the smallest BETi

An example with three drugs:
changing the number of NK cells
in the cancer tissue

PNAS

Complex role of NK cells in regulation of oncolytic virus–bortezomib therapy

Yangjin Kim[a,b,1], Ji Young Yoo[c,1], Tae Jin Lee[c], Joseph Liu[d], Jianhua Yu[e], Michael A. Caligiuri[f], Balveen Kaur[c,2], and Avner Friedman[a,g,2]

[a]Mathematical Biosciences Institute, The Ohio State University, Columbus, OH 43210; [b]Department of Mathematics, Konkuk University, Seoul, 143-701, Republic of Korea; [c]Department of Neurosurgery, University of Texas Health Science Center at Houston, Houston, TX 77030; [d]Department of Neurological Surgery, The Ohio State University Wexner Medical Center, Columbus, OH 43210; [e]Division of Hematology, Department of Internal Medicine, The Ohio State University Wexner Medical Center and The Ohio State University Comprehensive Cancer Center, Columbus, OH 43210; [f]Division of Administration, City of Hope National Medical Center, Duarte, CA 91010; and [g]Department of Mathematics, The Ohio State University, Columbus, OH 43210

June 2018

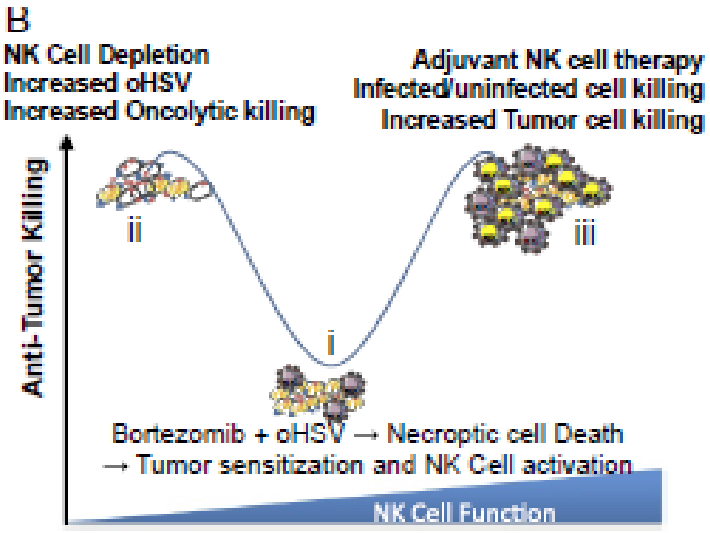

Fig. 5. (*A*) Experimental results: Kaplan–Meier survival curves of mice treated with bortezomib (Bort) and oHSV with or without adjuvant NK cell therapy. Both NK cell depletion and NK cell adjuvant therapy significantly enhance antitumor efficacy of mice treated with both bortezomib and oHSV. (*B*) A model depicting the impact of bortezomib and oHSV combination therapy on NK cell activity in vivo.

The anti-tumor efficacy increases when the endogenous NK cells are depleted or when exogenous NK cells are injected

This was established by mice experiments and, independently, by a mathematical model.

Final conclusion

Before starting clinical trials with two or more drugs, a thought should be given to the possible interaction between the drugs